TEORIJSKA I PRIMENJENA MEHANIKA 6, pp. 103–114, 1980 UDK 539.

LARGE DEFLECTION FINITE ELEMENT ANALYSIS OF ARCHES

Ljupčo Lazarov

(Received December 1979)

1. Introduction

In the conventional linear structural analysis any equilibrium equations used are applicable to the undeformed structural configuration in which case the compatibility equations neglect higher order effects in the deflections. A very pronounced effect of change of geometry on the structural behaviour is the buckling phenomenon, resulting in a loss of carrying capacity of the structure. In the case of large deflections, stresses exist which in the presence of certain displacements exert a significant influence on structural stiffness. The existence of axial loading in the presence of bending displacement effects the stiffness of the member. If the loading is compressive and approaches the critical value, the bending stiffness tends toward zero.

In order to develop a general method for an analysis of arches of any geometry and boundary condictions, a numerical technique must be used. The finite element method is a very powerful tool in analysing a geometric nonlinear formulation.

Here, a nonlinear displacement formulation is presented to analyse the elastic buckling and post-buckling behavior of archen. In particular, the curved beam element stiffness matrix is developed for the nonlinear buckling analysis (snap-through). The curved beam is formulated from the viewpoint of total potential energy, which leads to the development of the linear, incremental stiffness matrices for the elәment. The solution algorithm adopted is an iterative one, using a moving local coordinate system for each element.

The descending branch of the load-deflection curve in the post-buckling region is characterized by a nonpositive definite stiffness matrix. To evercome this difficilty an augmented stiffness scheme is used [1]. Adding linear springs with large stiffness in the direction of the applied forces the stiffness of the structure is artificially augmented. In the last section two examples are presented using the computer program *NONLIN* developed by the author et. al [2].

2. Stiffness Matrices for a Planar Curved Beam Element

The approximate expression for the strain in a prismatic beam element is given by,

$$\varepsilon = u_x + \frac{1}{2} v_x^2 - y v_{xx} \tag{1}$$

where: u = axial displacement, v = lateral displacement, normal to the longitudinal axis of the member, y = distance from the centroid of the cross section to any fiber, and where subscript x denotes partial differentiation. In the above expression the strain component $\frac{1}{2} u_x^2$ is neglected as smaller in comparison with the first term of the expression u_x. Nonlinear terms in the radius of curvatuve due to bending and shearing deformations are also ignored.

We shall assume that displacements u and v can be divided into deformational and rigid body components as follows:

$$u = u^d + u^{rb}, \quad v = v^d + v^{rb} \tag{2}$$

Substituting into the expression for the strain gives,

$$\varepsilon = u_x^d + \frac{1}{2} (v_x^d)^2 - y v_{xx}^d + v_x^d v_x^{rb} + u_x^{rb} + \frac{1}{2} (v_x^{rb})^2 - y v_{xx}^{rb} \tag{3}$$

The last three terms of (3) together represent the strain due to rigid body displacements which is zero. For convenience we shall drop the superscript d which denotes deformational displacement. Also let $v^{rb} = \bar{v}$, which can be interpreted as some initial deformed shape of the element. Thus, the approximate deformational strain is:

$$\varepsilon = u_x + \frac{1}{2} v_x^2 - y v_{xx} + v_x \bar{v}_x \tag{4}$$

To develop the element stiffness matrix we consider the following four deformational degrees of freedom: end rotations q_3 and q_6 and axial extensions w and q_4, fig. 1. Axial deformation w is included at midspan to enable

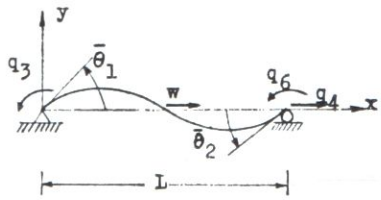

Fig.1

a linear variation of axial strain component u_x. The initia l deformed shape is defined through the end angles $\bar{\theta}_1$ and $\bar{\theta}_2$. Third order Hermitian polynomials are used in the initial deformed geometry $\bar{v}$ and the transverse displacement

shape function v [3]. For the longitudinal displacements a quadratic shape function is used. Now, the displacements u and v and the initial geometry of the element in local, element coordinate system are given through the nodal displacements and the angles $\bar{\theta}_1$ and $\bar{\theta}_2$ as follows:

$$
\begin{aligned}
u &= (4\xi - 4\xi^2)\, w + (2\xi^2 - \xi)\, q_4 \\
v &= (L(\xi^3 - 2\xi^2 + \xi)\, q_3 + L(\xi^3 - \xi^2)\, q_6 \\
\bar{v} &= L(\xi^3 - 2\xi^2 + \xi)\, \bar{\theta}_1 + L(\xi^3 - \xi^2)\, \bar{\theta}_2
\end{aligned} \tag{5}
$$

where $\xi = x/L$.

To complete the 6×6 element stiffness matrix using 4 deformational degrees of freedom: q_3, q_6, q_4 and w, we proceed as follows:

1. Determine thə expression for the strain energy U of the beam element retaining second order terms in q_3, q_4, q_6 and w. Linear elasɟicity is assumed, i.e. $\delta = E\varepsilon$

2. From the principle of minimum potential energy, we develop the element force-displacement ralationship. The linear incremental stiffness matrix is hence determined.

3. Condense out the axial degree of freedom w using static condensatiog procedure.

4. Expand 3×3 stiffness matrix to full 6×6 form by relating total displacements to deformational displacement components.

Proceeding to the foregoing outline we have,

$$
U = \frac{1}{2} E \int_0^L \left(\int_A \varepsilon^2 \, dA \right) dx \tag{6}
$$

where ε is as in expression (4).

The strain energy expression after expansion is

$$
\begin{aligned}
U = \frac{1}{2} E \int_0^L \Bigg[\int_A \Big(& u_x^2 + \frac{1}{4} v_x^4 + y^2 v_{xx}^2 + (v_x \bar{v}_x)^2 + u_x v_x^2 - 2 y u_x v_{xx} \\
& + 2 u_x v_x \bar{v}_x - y v_x^2 v_{xx} + v_x^3 \bar{v}_x - 2 y v_{xx} v_x \bar{v}_x \Big) dA \Bigg] dx
\end{aligned} \tag{7}
$$

The integrals of the form $\int y dA$ vanish since y is measured from the neutral axis and some more simplifications of the neutral axis and some more simplifications of the expression (7) can be done.

1. v_x^4: This term may be neglected since it contains nodal displacements to the fourth power.

2. $v_x^3 \bar{v}_x$: This term may be neglected since contains nodal displacements to the third power.

3. $u_x^2 + y^2 v_{xx}^2$: These terms lead to the usual linear stiffness matrix for a straight beam element.

4. $u_x v_x^2$: This term is third order in nodal displacements and leads to the geometric stiffness matrix. This term is neglected for the present.

5. $2 u_x v_x \bar{v}_x + (v_x \bar{v}_x)^2$: These terms lead to the portion of the stiffness matrix which account for initial element curvature.

Thus, to second order terms in nodal displacements, we have,

$$U = \frac{1}{2} E \int_0^L \left[\int_A (u_x^2 + y^2 v_{xx}^2 + 2 u_x v_x \bar{v}_x + (v_x \bar{v}_x)^2) \, dA \right] dx \tag{8}$$

Differentiating and substituting expressions (5) into the strain energy (8) and performing the interation we get,

$$U = \frac{EA}{L}\left(\frac{8}{3} w^2 - \frac{8}{3} w q_4 + \frac{7}{6} q_4^2\right) + \frac{2EI}{L}(q_3^2 + q_3 q_6 + q_6^2) +$$

$$+ EA\left[\frac{4}{15}\bar{\theta}_1 w q_3 - \frac{4}{15}\bar{\theta}_2 w q_6 -\right.$$

$$\left. - \frac{1}{30}\bar{\theta}_2 q_3 q_4 + \left(-\frac{1}{30}\bar{\theta}_1 + \frac{4}{15}\bar{\theta}_2\right) q_4 q_6\right] + EA\left[\frac{1}{420} q_3^2 L (12\bar{\theta}_1^2 - 3\bar{\theta}_1 \bar{\theta}_2 + \bar{\theta}_2^2) +\right.$$

$$\left. + \frac{1}{420} q_3 q_6 L (-3\bar{\theta}_1^2 + 4\bar{\theta}_1 \bar{\theta}_2 - 3\bar{\theta}_2^2) + \frac{1}{420} q_6^2 L (\bar{\theta}_1^2 - 3\bar{\theta}_1 \bar{\theta}_2 + 12\bar{\theta}_2^2)\right] \tag{9}$$

Applying the principle of minimum potential energy, the following force-deflection relationship results,

$$EA \begin{bmatrix} \frac{7}{3L} & \frac{-1}{30}\bar{\theta}_2 & & \\ \frac{4I}{AL} + \frac{L}{210}(12\bar{\theta}_1^2 - 3\bar{\theta}_1 \bar{\theta}_2 + \bar{\theta} & \frac{2I}{AL} + & & \\ \text{symmetric} & \frac{4I}{AL} + & & \\ \frac{1}{30}(-\bar{\theta}_1 + 8\bar{\theta}_2) & \frac{-8}{3L} & & \\ + \frac{L}{420}(-3\bar{\theta}_1^2 + 4\bar{\theta}_1 \bar{\theta}_2 - 3\bar{\theta}_2^2) & \frac{4}{15}\bar{\theta}_1 & & \\ + \frac{L}{210}(\bar{\theta}_1^2 - 3\bar{\theta}_1 \bar{\theta}_2 + 12\bar{\theta}_2^2) & \frac{-4}{15}\bar{\theta}_2 & & \\ & \frac{16}{3L} & & \end{bmatrix} \begin{Bmatrix} q_4 \\ q_3 \\ q_6 \\ w \end{Bmatrix} = \begin{Bmatrix} p_4 \\ p_3 \\ p_6 \\ p_w \end{Bmatrix} \tag{10}$$

where p_4, p_3, p_6 and p_w are nodal forces in the direction of q_4, q_3, q_6 and w The condensation of the internal degree of freedom w results in a 3×3 element stiffnes matrix $[k^*]$. To

$$[k^*]=EA\begin{bmatrix} \frac{1}{L} & \frac{1}{30}(4\bar{\theta}_1-\bar{\theta}_2) & \frac{1}{30}(-\bar{\theta}_1+4\bar{\theta}_2) \\ \frac{4I}{AL}+\frac{1}{1050}(46\bar{\theta}_1^2-15\bar{\theta}_1\,\bar{\theta}_2+5\bar{\theta}_2^2) & \frac{2I}{AL}+\frac{L}{700}(-5\bar{\theta}_1^2+16\bar{\theta}_1\,\bar{\theta}_2-5\bar{\theta}_2^2) & \\ \text{symetric} & \frac{4I}{AL}+\frac{L}{1050}(5\bar{\theta}_1^2-15\bar{\theta}_1\,\bar{\theta}_2+46\bar{\theta}_2^2) & \end{bmatrix} \tag{11}$$

expand this 3×3 element stiffness matrix which includes deformational degress of freedom only, we have to involve the three rigid body displacements. This results in

$$[k]=[t]^T[k^*][t] \tag{12}$$

$[t]$ being transformation matrix enabling us to convert deformational degrees of freedom $\{q^d\}$ into total set of displacements $\{q\}$

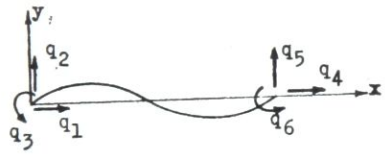

Fig.2

$$\{q^d\}=[t]\{q\} \tag{13}$$

$$[t]=\begin{bmatrix} -1 & 0 & 0 & 1 & 0 & 0 \\ 0 & \frac{1}{L} & 1 & 0 & -\frac{1}{L} & 0 \\ 0 & \frac{1}{L} & 0 & 0 & -\frac{1}{L} & 1 \end{bmatrix} \tag{14}$$

$$\{q^d\}=\begin{Bmatrix} q_4^d \\ q_3^d \\ q_d^6 \end{Bmatrix}\{q\}=\begin{Bmatrix} q_1 \\ q_2 \\ q_3 \\ q_4 \\ q_5 \\ q_6 \end{Bmatrix}$$

The resulting tangent stiffness matrix $[k]$ is divided into two parts: the usual linear stiffnes matrix $[k_L]$ for a straight beam element and that due to the initial curvature of the element $[k_C]$.

$$[k]=[k_L]+[k_C] \tag{15}$$

$$(16)\qquad [k_C] = EA \begin{bmatrix} \frac{1}{L} & 0 & 0 & -\frac{1}{L} & 0 & 0 \\ & \frac{12I}{AL^3} & \frac{6I}{AL^2} & 0 & -\frac{12I}{AL^3} & \frac{6I}{AL^2} \\ & & \frac{4I}{AL} & 0 & -\frac{6I}{AL^2} & \frac{2I}{AL} \\ & & & \frac{1}{L} & 0 & 0 \\ & & & & \frac{12I}{AL^3} & -\frac{6I}{AL^2} \\ & \text{symmetric} & & & & \frac{4}{I} \end{bmatrix}$$

and $[k_C]$ is swown on the following page (17).

As previously stated, the term $u_x v_x^2$ in the the strain energy exspression given rise to the geometric stiffness matrix. Since quadratic function for u has been assumed (hrough the introduction of the midspan axial of freedom w), the consistent evaluation of the geometric stiffness matrix becomes somewhat complicated. However, the obtained results using consistant geometric stiffness matrix do not show any improvement over the results obtained using linear variation for u in the development of the geometric stiffness matrix. For the sake of this the familiar geometric stiffness matrix derived in reference [4] is used throughout this study, expression (18)

$$[k_C] = EA \begin{bmatrix} 0 & \frac{-1}{10L}(\bar{\theta}_1 + \bar{\theta}_2) & \frac{-1}{30}(4\bar{\theta}_1 - \bar{\theta}_2) & 0 \\ & \frac{3}{175L}(2\bar{\theta}_1^2 + \bar{\theta}_1\bar{\theta}_2 + 2\bar{\theta}_2^2) & \frac{1}{2100}(77\bar{\theta}_1^2 + 18\bar{\theta}_1\bar{\theta}_2 - 5\bar{\theta}_2^2) & \frac{1}{10L}(\bar{\theta}_1 + \bar{\theta}_2) \\ & & \frac{L}{1050}(46\bar{\theta}_1^2 - 15\bar{\theta}_1\bar{\theta}_2 + 5\bar{\theta}_2^2) & \frac{1}{30}(4\bar{\theta}_1 - \bar{\theta}_2) \\ & & & 0 \\ & \text{symmetric} & & \end{bmatrix}$$

$$
\begin{bmatrix}
 & \frac{1}{10L}(\bar{\theta}_1+\bar{\theta}_2) & & \frac{-1}{30}(-\bar{\theta}_1+4\bar{\theta}_2) \\
\frac{-3}{175L}(2\bar{\theta}_1^2+\bar{\theta}_1\bar{\theta}_2+2\bar{\theta}_2^2) & & \frac{2}{2100}(-5\bar{\theta}_1^2+18\bar{\theta}_1\bar{\theta}_2+77\bar{\theta}_2^2) & \\
\frac{-1}{2100}(77\bar{\theta}_1^2+18\bar{\theta}_1\bar{\theta}_2-5\bar{\theta}_2^2 & & \frac{L}{700}(-5\bar{\theta}_1^2+16\bar{\theta}_1\bar{\theta}_2-5_2^2) & \\
 & -\frac{1}{10L}(\bar{\theta}_1+\bar{\theta}_2) & & \frac{1}{30}(-\bar{\theta}_1+4\bar{\theta}_2) \\
\frac{3}{175L}(2\bar{\theta}+\bar{\theta}_1\bar{\theta}_2+2\bar{\theta}) & & \frac{-1}{2100}(-5\bar{\theta}_1^2+18\bar{\theta}_1\bar{\theta}_2+77\bar{\theta}_2^2) & \\
 & & \frac{L}{1000}(5\theta_1^2-15\bar{\theta}_1\bar{\theta}_2+46\bar{\theta}_2^2) &
\end{bmatrix}
$$

$$
[k_G]=\frac{F}{L}\begin{bmatrix}
0 & 0 & 0 & 0 & 0 & 0 \\
 & \frac{6}{5} & \frac{L}{10} & 0 & -\frac{6}{5} & \frac{L}{10} \\
 & & \frac{2L^2}{15} & 0 & -\frac{L}{10} & -\frac{L^2}{30} \\
 & & & 0 & 0 & 0 \\
 & \text{symmetric} & & & \frac{6}{5} & -\frac{L}{10} \\
 & & & & & \frac{2L^2}{15}
\end{bmatrix} \tag{18}
$$

where F denotes the axial force in the element, calculated from the change in element length after deformation.

3. Solution Algorithm

The algorithm for the solution used in this study is based on the linear incremental iterative solution method with moving coordinates [5], [6], [7]. Some authors prefer to name it update Lagrangean or Eulerian formulation [8]. Basically it means that the full load range is divided into small load increments applied once at a time defining the state of the forces and deformations in the structure after that load increment. When the next load increment is applied we actually solve a new linear problem with a configuration and initial stresses preserved after the previous load increment applied. Following this technique we solve even a highly nonlinear problem by dividing-the whole load range into many linear sequences. An essential requirement, however, is that the elements be small enough so that relative rotations in each element local coordinate system are small. To satisfy this requirement a fine mesh of elements is required for large load increments, or alternatively rather small

load increments applied to a rough mesh. More details about this formulation can be found in the following references [5] [9], [10], [11].

The iterative solution using the foregoing incremental structural equations is an application of the Newton-Raphson method for solving algebraic equations [22]. During the solution process the structural stiffnes matrix is updated in each iteration, resulting in a fast convergence even in cases with severe nonlinearity [12], [10], [13].

A tupical iteration cycle can be described as follows::

Suppose we have achieved equilibrium satisfied within the limits of a required accuracy for a given expernal load level $\{P_i\}$ and that we have determined all elements internal forces $\{F\}_i^e$ coresponding to this load level. $\{D\}_i$ are total displacements in this deformed configuration. To reach the structure response for a load level $\{P\}_{i+1}=\{P\}_i+\{\Delta P\}$, $\{\Delta P\}$ being load increment vector, we proceed as follows:

1. Determine each element stiffness matrix $[k]^e$ for the last deformed configuration

$$[k^e]=[k_L]^e+[k]_C^e+[k_G]^e$$

and assemble structure tangent stiffness matrix $[K]=\sum[k]^e$

2. Solve incremental structural equations

$$[K]\{\Delta D\}=\{\Delta P\}$$

for displacement increments $\{\Delta D\}$.

3. Update total displacements up to date $\{D\}_{i+1}=\{D\}_i+\{\Delta D\}$. Create the total load $\{P\}'_{i+1}$ at the present position coresponding to displacement $\{D\}_{i+1}$.

4. Test for convergence. In this stupy a displacement convergence criterion is used [14]. For each structural degree of freedom, i, the ratio $e_i=|\Delta D_i/D_{iref}|$ should be less than a specific limit, depending upon the accuracy required. Iu this criterion ΔD_i is the most recently computed displacement increment and D_{iref} is the largest total displacement within the current load step of the same type. For example, if ΔD_i is a rotation increment, D_{iref} is the largest nodal rotation in the structure accumulated within all previous iterations of the given load increment.

If convergence is not accomplished the next load increment vector is obtained as $\{\Delta P\}'=\{P\}_{i+1}-\{P\}'_{i+1}$ and restart the procedure from step 1.

If the convergence is in a specific limit we go to a new load increment $\{\Delta P\}$ and search for a new epuilibrium position at load level $\{P\}_{i+2}=\{P\}_{i+1}+\{\Delta P\}$ starting from step 1.

4. Results. In this section two shallow circular arch example are presented. For both of them the complete highly nonlinear loaddflection curve is obtained and the results are compared with existing solutions presenthed in the literature.

A Pinned Circular Shallow Arch. The following material and geometric properties are assigned as they are shown in Fig. 3: span $L=254$ cm, rise $h=7{,}62$ cm, width of the arch $b=2{,}54$ cm, the thickness $\delta=7{,}62$ cm, elasticity modulas $E=6{,}895\times10^{11}\ N/m^2\cdot k$ is a stiffness of a linear spring under the concentrated applied load P, $k=1751$ kN/cm*.

* All input data for both examples are obtained when reference solution input data from [1], [7], [15] and [16] are converted into SI Metric Units.

Such a large stiffness for k results in a dispacements controlled solution and makes the structural stiffness matrix positive defined in the entire range of the load-displacement curve. In this example only symmetric buckling is considered. Half of the arch is devided in 8 curved beam elements and the displacement of the centre point is incremented to allow a study of snapthrough behaviour. Twenty load increments are applied to get the plot in Fig. 3 using

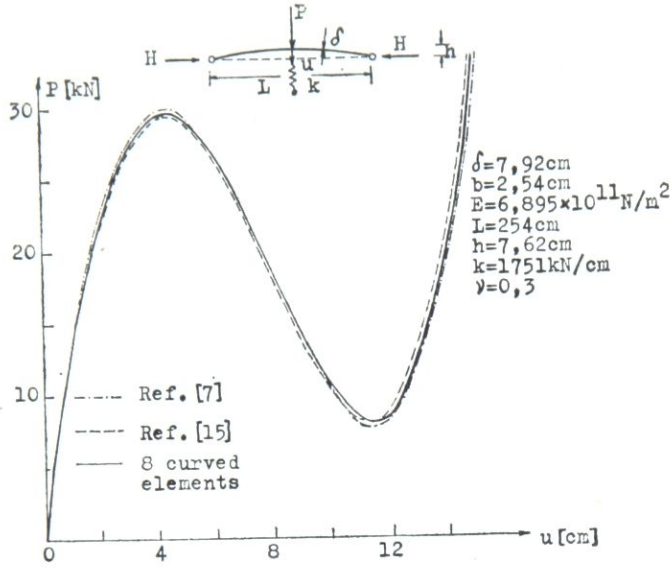

Fig.3- A PINNED CIRCULAR SHALLOW ARCH

8 elements. Almost the same results are obtained when 16 elements are used. The problem was run on the CYBER 175 computer at the University of Illinois, Urbana-Champaign. The approximate *CP* time was 0,01875 sec. per element per a load increment with a displacement convergence tolerance $e = 10^{-6}$ requiring approximately 5 iterations per a load increment. An excellent agreement was obtained with the closed solution of ref. [15], and the isoparametric finite element solution of Zienkiewicz and Nayak, ref [7] with 10 parabolic plane elements. It is worthnoting that even using only 4 elements the obtained results were fairly adequate to get an astimate of the critical force P. The applied loadhorizontal thrust curve (P-H) is presented in Fig. 4.

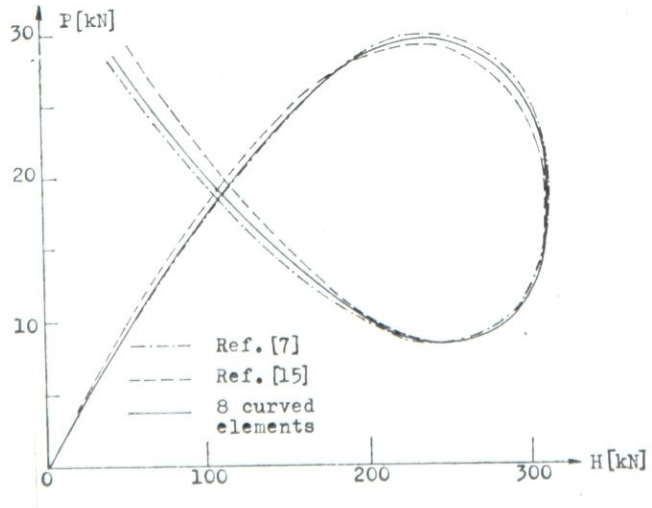

Fig.4-APPLIED LOAD-HORIZONTAL THRUST CURVE

A Clamped Circular Shallow Arch. A snap-through behaviour of a clamped circular shallow arch is analyzed, Fig. 5, and compared with the coressponding closed solution [16] and with the finite element method solution obtained by Sharifi and Popov [1]. The properties of the arch are: radius of curvature $R = 254$ cm, central angle $2\beta = 1{,}414$ rad, width $b = 2{,}54$ cm, thickness $\delta = 5{,}08$ cm and elasticity modulas $E = 6{,}895 \times 10^{11}$N/m^2. The coresponding span is $L = 329{,}97$, cm and rise $h = 60{,}88$ cm. A concentrated load P is applied at the central point and a spring with a linear stiffeness $k = 1751$ kN/cm under the load. Only half of the arch is analyzed for the case of symmetrical buckling using 8 curved beam elements. The load is applied in 8 increments. The

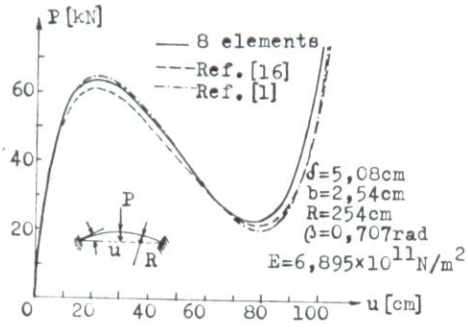

Fig.5-A CLAMPED SHALLOW ARCH

load-central deflection plot is given in Fig. 5. The solution from ref. [1] was obtained using 11 staight beam-column type elements within the half span of the arch, with element stiffness matrix being derived considering: flextural, extensional and shear deformations. As is mentioned in ref [1] the approximate computer time on the *CDC* 6400 equipment was 0,075 sec. per element per lod increment or a total of $0{,}075 \times 11 \times 69 = 56{,}92$ sec *CP* time, 69 being the number of load increments. In the present study results with comparab'e accuracy were obtained for approximately $0.0185 \times 8 \times 80 = 11{,}84$ sec *CP* time. Transverse displacements along the arch are plotted in Fig. 6.a after the 10 th, 20 th, 40 th, and 80 th load increments applied. Bending moment diagrams after the 4 th, 60 th, and 80 th load increments are given in Fig. 6 b.

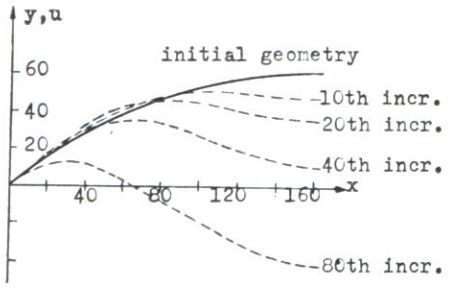

Fig.6a-TRANSVERSE DISPLACEMENTS

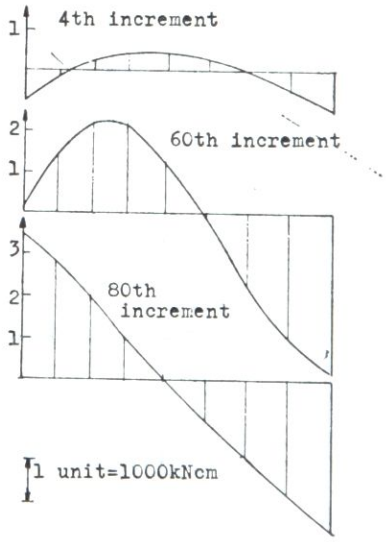

Fig.6b-BENDING MOMENTS

REFERENCES

[1] Sharifi, P. and Popov, E.P., *Nornlinear Buckling Analysis of* Sandwich Arches, Journal of the Eng. Mech. Div., EM 5, Oct. 1971

[2] Lazarov, L., Nau, J. and Morrison, D.G., Planar, *Curved Beam Element for Analysis of Shallow Arches, Students Report*, U of I, 1979

[3] Glaum, L.W., *Direct Iteration and Perturbation Methods for* the *Analyysis of Nonlinear Structures*, PhD Thesis, University of Illinois Chicago Circle, 1976

[4] Przemieniecki, J.S., *Theory of Matrix Structural Analysis*, McGraw-Hill, 1968

[5] Cook, R.D., *Concepts and Applications of Finite Element Analysis*, John Wiley, 1974

[6] Mallett, R.H. and Marcal, P.V., *Finite Element Analysis of Nonlinear Structures*, Journal of Str. Div., ST 9, Sept 1968

[7] Zienkiewicz, O.C. and Nayak, G.C., *A Genaral Approach to Problems of Plasticity and Large Deformation Using Isoparametric Elements*, Proc. of the Third Conf. on Matrix Methods in Struct. Mech., Wright-Patterson Air Force Base, Ohio, Oct., 1971

[8] Cescotto, S., Frey, F. and Fonder, B., *Total and Updated Lagrangian Descriptions in Nonlinear Structural Analysis:* A Unified Approach from: Energy Methods in Finite Element Analysis, edited by Zenkiewicz and Rodin, 1979

[9] Haisler, W.E., Stricklin, J.A. and Stebbins, F.J., *Development and Evaluation of Solution Procedures for Geometrically Nonlinear Structural Analysis*, AIAA Journal, Vol. 10, N°. 3. March 1972

[10] Stricklin, J.A., Haisler, W.E. and Reisemann, W.A., *Evaluation of Solution Procedures for Material and/or Geometrically Nonlinear Structural Analysis*, AIAA Journal, Vol. 11, N°. 3, March 1973

[11] Murray, D.W, and Wilson, E.L., *Finite Element Deflection Analysis of Plates*, Journal of the Eng. Mech. Div., EM 1, Feb. 1969

[12] Scarborough, J.B., *Numerical Mathematical Analysis*, Oxford University Press, 1966

[13] Oden, J.T., *Finite Elements of Nonlinear Continua*, McGraw-Hill, New York, 1972

[14] Bergan, P.G. and Clough, R.W., *Convergence Criteria for Iterative Processes*, AIAA Journal, Vol. 10, N°. 8, Aug. 1972

[15] Biezeno, C.B. and Grammel, R., *Elastic Problems of Single Machine Elements*, Van Nostrand, 1956

[16] Schreyer, H. and Masur, E., *Buckling of Shallow Arches*, Journal of the Eng. Mech. Div., EM 4, Aug. 1966

GRANDS DÉPLACEMENT DES ARCH ANALYSÉS PAR LA MÉTHODE

Ljupčo Lazarov

Rèsumè

Dans cet article une formulation nonlinéaire dans les dèformations est présentée, pour une analyse de flambage d'un arc de geometrie généralle. Particilièrement la matrice de la rigiditée pour un element courb est développée. La méthode de solution est une iterative incremental utilisant un système des cordinates qui se changent avec la change de la configuration de la construction dans le procès de la déformation.

VELIKA POMERANJA LUKA ANALIZIRANA METODOM KONAČNIH ELEMENATA

Ljupčo Lazarov

Izvod

U ovom radu prikazana je nelinearnd formulacija deformacija u cilju analize savijanja luka opšteg oblika. Posebno je razvijena matrica krutosti za krov element luka. Rešenje je dobijeno metodom iterativnih priraštaja, a korišćen je koordinatni sistem koji se menja sa promenom konfiguracije konstrukcije u procesu deformacije.

Ljupčo Lazarov
Gradežen fakultet
Rade Končar, 16
91000 — SKOPJE